REPORT

MATERIALS SCIENCE

Centrifugation and index matching yield a strong and transparent bioinspired nacreous composite

Ali Amini[1,2], Adele Khavari[1]†, Francois Barthelat[2,3], Allen J. Ehrlicher[1,2,4,5,6,7]*

Glasses have numerous applications because of their exceptional transparency and stiffness; however, poor fracture, impact resistance, and mechanical reliability limit the range of their applications. Recent bioinspired glasses have shown superior mechanical performance, but they still suffer from reduced optical quality. Here, we present a nacreous glass composite that offers a combination of strength, toughness, and transparency. Micrometer-sized glass tablets and poly(methyl methacrylate) (PMMA) were mixed and structured by centrifugation, creating dense PMMA-glass layers. A transparent composite was created by tuning the refractive index of PMMA to that of glass and using chemical functionalization to create continuous interfaces. The fabrication method is robust and scalable, and the composite may prove to be a glass alternative in diverse applications.

Engineering glasses are brittle materials with low fracture toughness (the material's capability to resist the growth of a crack or flaw) and low strength (the material's resistance against failure), which limits the range of their applications (*1*). Thermal or chemical tempering is a common strategy used to increase the strength of glasses (*2*); however, this does not markedly improve fracture toughness (*3*) and can lead to catastrophic, "explosive" types of failures. Laminating creates a polymeric glass sandwich-like composite structure (*4*), the greatest advantage of which is safety: Upon fracture, the polymeric layers prevent small pieces of fractured glass from shattering in catastrophic failure. However, there are only modest mechanical improvements observed in laminated glasses (*5–7*).

To improve glass toughness and strength, researchers have explored implementing design principles observed in biology. Nacre, the tough material that makes up the inner layer of mollusk shells, is a classic example of a tough structural biomaterial. Nacre is 3000 times as tough as its individual constituents (*8*); it breaks at 1% of strain, which is substantially higher than the individual ceramic building blocks; and its elastic modulus is ~1000 times as large as that of the connective proteins alone (*9*).

Many techniques of varying complexity have been proposed to fabricate synthetic materials mimicking nacre's structure (*10*, *11*). Some of these have focused on making transparent composites (*12–14*), resulting in thin films with enhanced mechanical and optical properties. To extend the applications beyond thin films, a scalable nacreous composite has been developed by infiltrating poly(methyl methacrylate) (PMMA) into a glass tablet scaffold while matching refractive indices of the two phases (*15*). Despite superior fracture resistance properties compared with glass, this composite is less transparent.

Others have used top-down methods, including laser-engraving interlocking jigsaw-shaped three-dimensional arrays in bulk glass (*16*) and glass lamination processes of thin glasses with laser-engraved cross-plied (*17*) and tablet-like architectures (*18*). These approaches have resulted in increased composite fracture toughness and impact resistance, but reduced stiffness and strength. Stiffness and strength can generally be improved by decreasing the size of the patterns; however, this reduces transparency and scalability (*18*). This highlights a general trade-off challenge that bioinspired glasses have suffered from between mechanics, transparency, and fabrication scalability.

The structure and composition of our transparent nacre-like material result from stringent requirements and careful material selection and preparation. For high mechanical performance—i.e., high toughness, strength, and stiffness—hard and stiff inclusions with high aspect ratios must be bonded by a more deformable and weaker matrix (*9*, *19–22*). For high optical performance, the refraction index of the two phases must be identical. Finally, a strong bonding between the hard and soft phase is required to ensure a high level of interface strength and to prevent light scattering that would reduce optical quality. To fulfill these mechano-optical requirements, we chose micrometer-sized glass tablets (64 to 70% SiO_2; detailed chemical composition is described in the supplementary materials) for the hard inclusions and PMMA for the soft matrix. Glass tablets were utilized as the hard component because of their high diameter-to-thickness aspect ratio, transparency, high stiffness, and well-characterized surface chemistry for surface functionalization. PMMA, an amorphous polymer that polymerizes through a free radical bulk polymerization process (*23*), was selected as the soft phase because of its deformability (*24*) and excellent optical properties (*25*). The optical refraction indices of glass ($n_{glass} = 1.52$) and PMMA ($n_{PMMA} = 1.49$) do not exactly match, but they can be made to do so by adding an organic dopant, phenanthrene, to PMMA (*26*).

To achieve a strong and defect-free interface between glass and PMMA, we functionalized the glass tablet surface with a silane [(3-trimethoxysilyl)propyl methacrylate, or γ-MPS] (Fig. 1 and fig. S1). The prepared PMMA and glass tablets were mixed and then centrifuged to induce an aligned brick-and-mortar architecture and high volume fraction of glass inclusions. As a final stage, PMMA polymerization was achieved by baking at 50°C (for 12 hours), 70°C (for 4 hours), and 100°C (for 2 hours).

We measured the refractive index of PMMA-dopant samples as a function of dopant weight percentage (fig. S2A) and then estimated the composition that leads to the highest level of transparency (fig. S2D). Although the composite with no index-matching dopant was very hazy, and the sample was not transparent because of light scattering, our index-matched glass composite demonstrated high levels of transparency (Fig. 2A). The optical transmittance of our glass composite compares well with both soda-lime monolithic glass and PMMA doped with 12% phenanthrene, particularly in the sensitive spectrum of human vision (400 to 700 nm) (Fig. 2B), and its average transmittance is only 16% less than the soda-lime glass (fig. S2E). It also has 24% higher transmittance than similar bioinspired laminated composites (*18*) and has almost 100% higher transmittance than a nacre mimetic composite (*15*). (fig. S2, E and F). Although the method in (*15*) mimics other aspects of nacre by creating mineral bridges through a heat-treatment process, this process also creates many potential light-scattering sites, leading to the poor optical performance reported for that material. The pale yellow color of our composite is a result of the phenanthrene's molecular structure, which blocks a major part of the blue light. This is mainly because of the conjugation—alternating arrangement of single and double bonds between carbon atoms (*27*)—

[1]Department of Bioengineering, McGill University, Montreal, Quebec H3A 0C3, Canada. [2]Department of Mechanical Engineering, McGill University, Montreal, Quebec H3A 0C3, Canada. [3]Department of Mechanical Engineering, University of Colorado Boulder, Boulder, CO 80309, USA. [4]Department of Anatomy and Cell Biology, McGill University, Montreal, Quebec H3A 0C7, Canada. [5]Department of Biomedical Engineering, McGill University, Montreal, Quebec H3A 2B4, Canada. [6]Centre for Structural Biology, McGill University, Montreal, Quebec H3G 0B1, Canada. [7]Goodman Cancer Research Centre, McGill University, Montreal, Quebec H3A 1A3, Canada.
*Corresponding author. Email: allen.ehrlicher@mcgill.ca
†Present address: Michael Smith Laboratories, University of British Columbia, Vancouver, British Columbia, V6T 1Z4, Canada.
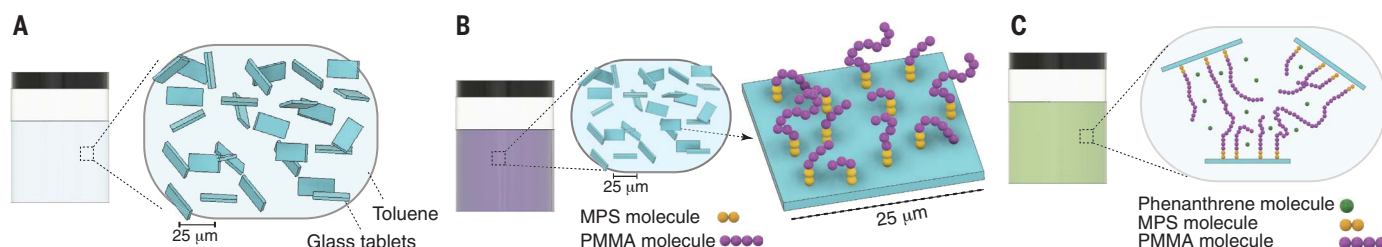
Fig. 1. Centrifuge-based fabrication method of nacreous glass composite. (**A**) Cleaned glass tablets were dispersed in toluene. (**B**) Glass tablets were surface treated with γ-MPS and then with a solution of MMA in toluene to promote polymerization from the glass surface. (**C**) Surface-treated glass tablets were involved in free radical polymerization of PMMA at 50°C.
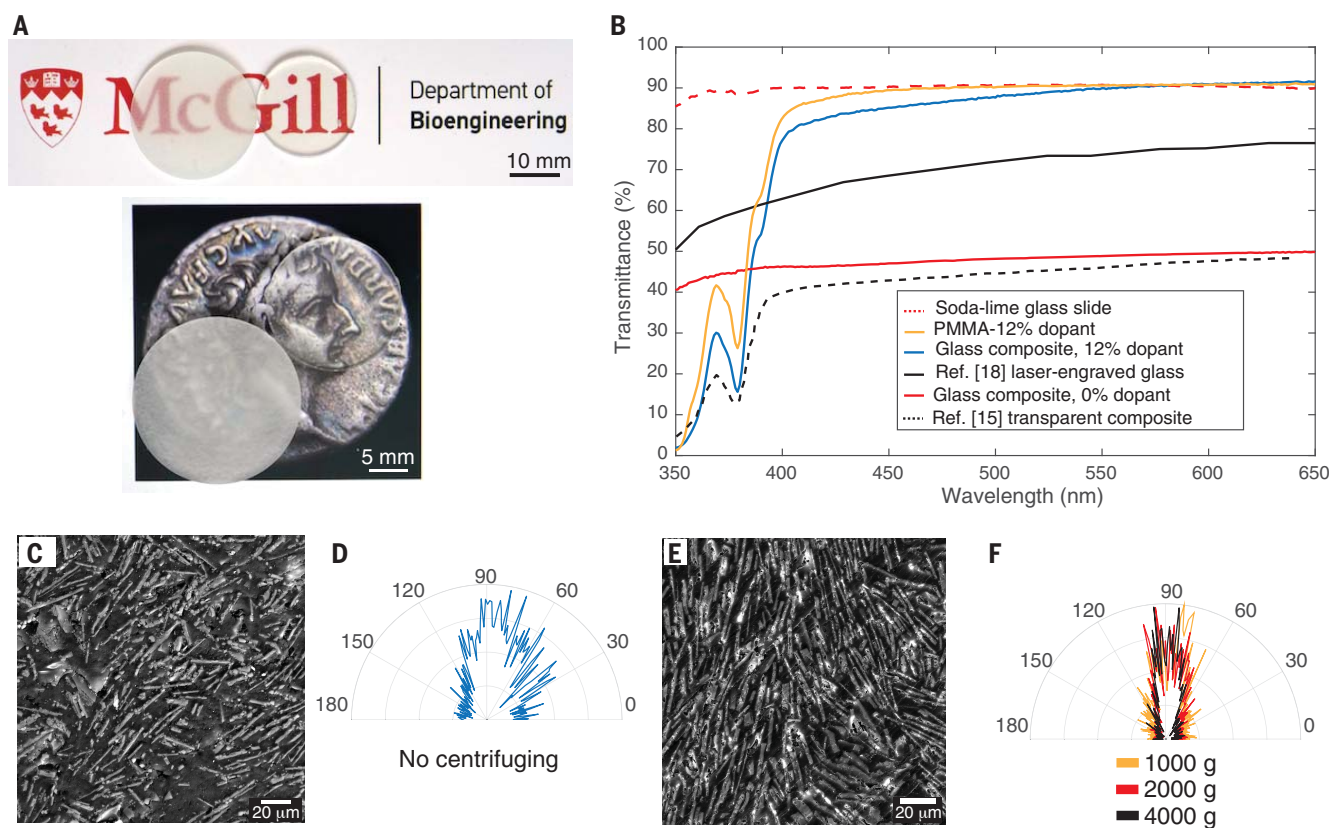

Fig. 2. Adding dopant yields a transparent composite, and centrifugation imposes order and compactness on the structure. (**A**) One-millimeter-thick glass composites with 0% dopant (samples on the left) and 12% dopant (samples on the right). The "Tribute Penny" coin is attributed under CC BY-SA 3.0. (**B**) Transmittance for the soda-lime glass, doped PMMA (12%), 12% glass composite, laser-engraved laminated glass (*18*), and bioinspired transparent composite (*15*). Transmittance values were measured at room temperature (20°C). (**C**) Section SEM image of a noncentrifuged composite (~24% glass volume fraction). We observed a noticeable number of areas with no tablets and also many tablets with random orientations in the material. (**D**) The distribution of tablet orientations also confirms this observation. (**E**) Section SEM image of centrifuged composite (2000*g*, ~43% glass volume fraction). Tablets are more oriented in one direction, and areas with no tablets are rarely observed. (**F**) Polar distribution of orientation in the tablets for different centrifuging speeds.

where the energy spacing between π and π* orbitals in a conjugated system matches the energy range associated with the visible light spectrum. As the conjugated systems become bigger, the maximum absorbance peak shifts to the larger wavelengths. To overcome this effect, one solution would be to use polycyclic aromatic hydrocarbons with smaller conjugated systems. We successfully tested biphenyl, as an example of a smaller conjugated system (fig. S3), and it does not block blue light; therefore, the resulting composite does not have a yellow tint.

In addition to high optical performance, our material needs to be stiff and possess high levels of tensile strength and fracture tough-ness, which requires a high concentration of well-aligned glass inclusions. As glass and PMMA have different densities, we used cen-trifugation to increase the fraction of glass in our composite, leading to a high volume fraction of the stiff (glass) phase and conse-quently a thin interstitial connective (PMMA) phase. The volume fraction of glass inclusions
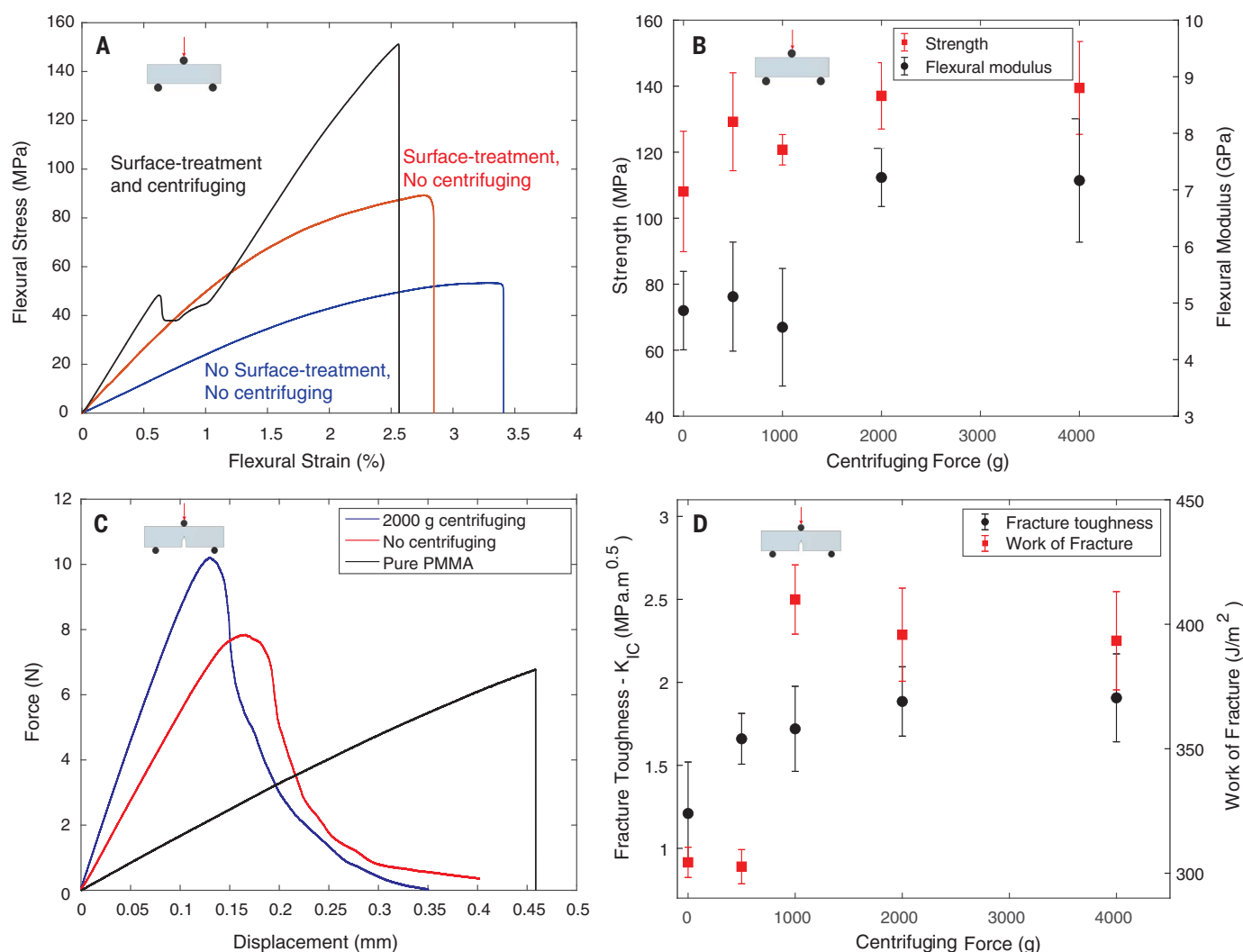
Fig. 3. Surface functionalization and centrifuging process improve the mechanical properties of the glass composite. (**A**) Flexural stress–flexural strain curves for the composites with and without surface-functionalized glass and centrifugation. (**B**) Strength and flexural modulus increase with centrifuga-tion. (**C**) SENB test load-displacement curves for pure PMMA, noncentrifuged, and centrifuged composites, illustrating an increased fracture strength with composite formulation and subsequent centrifugation. (**D**) K_{IC} and WOF values increase with increasing the centrifuging speed up to 2000g.

increased from ~24% for noncentrifuged com-posites to ~43% for the samples centrifuged with 2000g (fig. S4). The thickness of the polymer layer between the tablets also de-creased from ~35 μm for the simply mixed sample to ~17 μm for the sample centrifuged with 2000g. Centrifugation homogenizes the distribution of tablets, preventing the forma-tion of tablet-free regions of PMMA (Fig. 2, C and E). Centrifugation also aligns the glass tablets (Fig. 2, D and F). By comparing the polar orientation distribution graphs of the noncentrifuged and centrifuged composites, we examined the role of the centrifuging pro-cess in inducing order in the structure of the composite. Centrifugation up to 2000g in-creased tablet order and alignment; how-ever, further increasing the centrifugation speed did not seem to considerably improve

tablet alignment. Because no drastic change in volume fraction (or mechanical testing data, as in Fig. 3) was observed with further in-creasing the centrifuging speed, we determined 2000g to be an optimal centrifugation force.

The mechanical performance of the compo-site was evaluated using three-point bending tests. The glass composite displays two distinct linear and nonlinear regimes in flexural re-sponse (Fig. 3A). We attribute the nonlinear regime to the relatively large shear deforma-tion of PMMA, which enables the relative displacement of the glass tablet following the shear lag model (*28*). PMMA is considered to be brittle compared with other polymers; how-ever, it exhibits ductile behavior when com-pared with brittle materials such as glass and ceramics (fig. S5). Besides, PMMA is much more deformable in shear than in tension (*29*).

All samples displayed evidence of inelastic de-formation, with strains at failure in the 2.5-to-3.5% range. Flexural modulus and strength, however, varied significantly across the differ-ent designs we explored. The glass composite surface functionalized with γ-MPS was 1.9 times as stiff as the glass composite without any surface treatment (Fig. 3A and table S1). The composite's flexural strength increased about twofold by functionalizing the glass tablets' surfaces with γ-MPS. This increase in strength, however, only produced a glass com-posite slightly stronger than pure PMMA (table S1). The flexural strength increased to ~140 MPa by including the centrifuge process as a part of the fabrication process; this aligned the glass tablets into layers of parallel planes and also yielded a denser overall structure. The beneficial strengthening
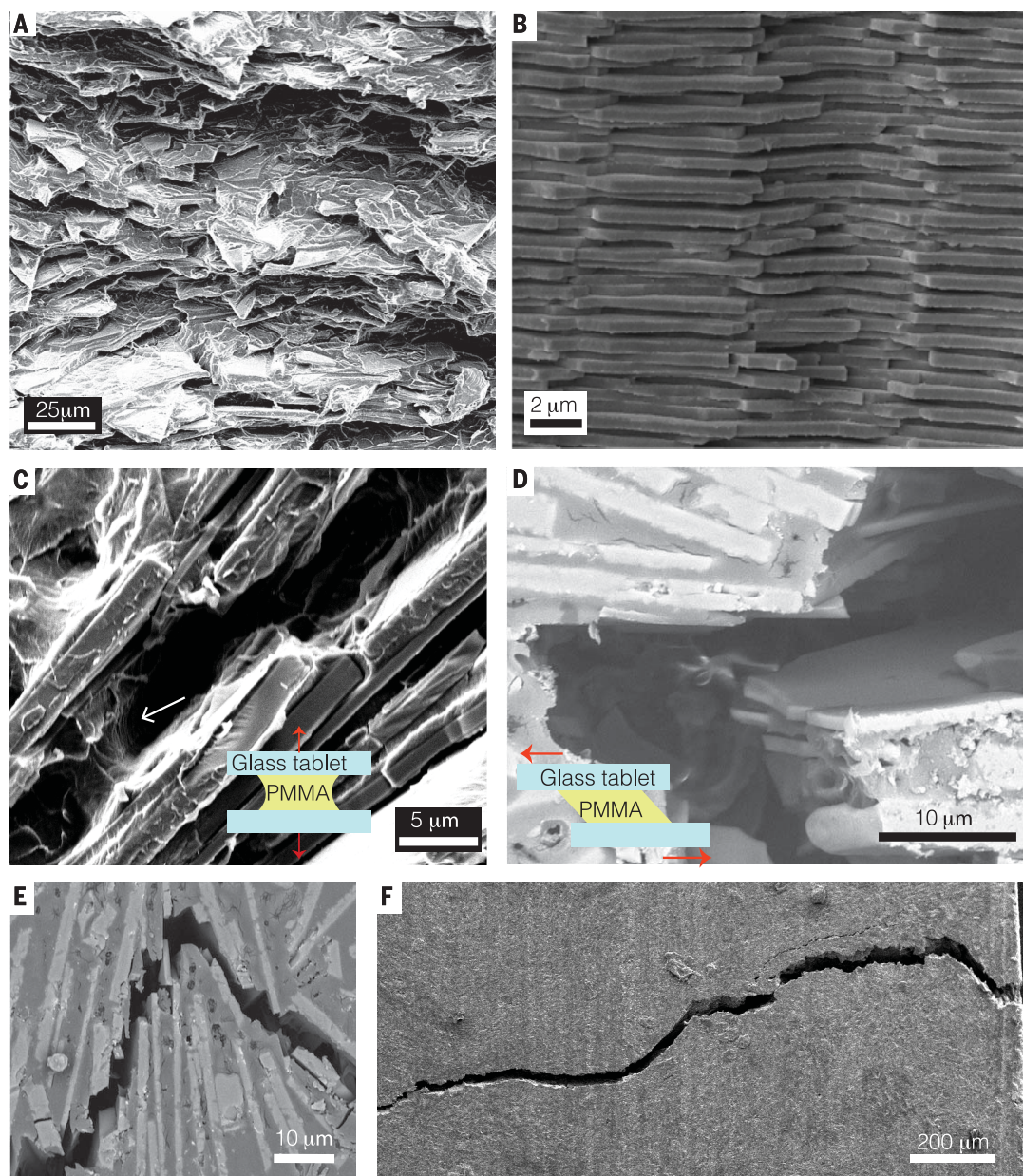
Fig. 4. Transparent nacreous glass mimics key aspects of nacre's microstructure and toughening mechanisms. (**A**) SEM micrograph of the sample cross section in a fractured surface in our glass composite. Staggered glass platelets with polymer layers in between and numerous pulled-out glass tablets are a result of fracture. (**B**) Fracture surface of natural nacre. (**C**) Whereas tablets are experiencing delamination as a result of lateral deformation, the polymer layer acts as a bridge between tablets and contributes to the composite toughness (white arrow). (**D**) Relative displacement of tablets as a result of shear loading. (**E**) Tablet pull-out and deflection of crack growth path in microscale. (**F**) Macroscopic crack deflection in the material as a result of microscopic toughening mechanisms.

effects of centrifugation appeared to plateau at 2000g, with no substantial increase in flexural strength for higher forces (Fig. 3B). The flexural modulus increased from 4.7 GPa for the noncentrifuged sample to ~7.2 GPa for the sample centrifuged with 2000g force, with no significant increase of the modulus with higher centrifugation speeds. The effect of surface functionalization and centrifugation appeared to be insignificant on the rupture strain, and most of the samples possessed a rupture strain of ~3% (fig. S6 and table S1).

In addition to modulus, strength, and deformability, we measured fracture toughness using a single-edge notch bending (SENB) configuration. Figure 3C shows typical force-deflection results for these tests, showing a brittle response for pure PMMA (indicating fast and catastrophic crack propagation with little toughening) but a more controlled and "graceful" failure with a more-gradual decrease in force in the postpeak region for the glass composite (indicating stable crack propagation associate with toughening mechanisms). The centrifuged glass composite also showed a higher peak force. We computed the fracture toughness K_{IC} using the maximum force in linear regime (*30*, *31*) and the work of fracture [(WOF) energy required to break a material into two parts as a result of fracture] from the area under the force-deflection curve. By centrifuging (2000g), we increased the glass com-

posite's fracture toughness (K_{IC}) and energy absorption (WOF) by ~55 and 30%, respectively (Fig. 3D). To demonstrate the behavior of the material in terms of crack propagation, we also computed the J integral values and derived the resistance curves (K_J, fracture toughness against crack extension length). A rising pattern in toughness values was observed as the crack propagated in the material (fig. S7C). The maximum K_J value before crack instability (K_{JC}, based on the criteria in eqs. S10- to S12) for the 2000g composite was ~4.51 MPa m$^{1/2}$ (~448.5 J/m^2). This was about twice the estimated K_{IC} value, which suggests that extrinsic toughening mechanisms are activated after crack growth starts.

The results in Fig. 3 demonstrate that centrifuging improves the mechanical and fracture properties. This improvement is achieved by inducing order in the structure and creating a staggered structure of glass tablets and PMMA polymer similar to the structure of nacre (Fig. 4, A and B). Such order promotes some important extrinsic toughening mechanisms, leading to the excellent performance of the composite under fracture.

In the absence of mineral bridges and tablet interlocking, a key toughening mechanism in our material is polymer bridging by the formation of polymer ligaments between tablets, activated when the delamination of tablets occurs (Fig. 4C and fig. S7). This mechanism occurred either by complete debonding (Fig. 4C and fig. S8, A and B) or by the formation of microscopic cavities in the soft phase (fig. S8, C and D). Also reported to occur in natural nacre (32), tablets experience delamination as a result of lateral displacements if (i) the interface material is deformable and (ii) the bonding between polymer and glass is strong (33). This highlights the role of glass surface treatment and consequent strong bonds between the soft and hard phases. The relative displacement of the individual tablets from local tensile stress and interfacial shear stresses (Fig. 4D) is another important micromechanism that not only absorbs energy through plastic deformations in the soft phase, but also leads to tablet pull-out—a mechanism that contributes to high levels of toughness in biological nacre (21) (Fig. 4, A and E, and fig. S9, A and B). Scanning electron microscopy (SEM) images suggest that crack deflection and delamination frequently occur, with crack deflection appearing to be a central toughening mechanism in our composite. Tablet pull-out, however, appears to occur less frequently. Previous models have shown that the WOF as a result of pull-out is directly proportional to the volume fraction of the hard phase (32), and therefore we attribute the less-frequent occurrence of tablet pull-out in our material to the relatively bigger polymer layer thickness and consequently lower volume fraction compared with natural nacre. Mechanisms such as crack deflection, however, give rise to large deformations, and high levels of energy absorption manifest as high fracture toughness in the material. Because of the activation of the toughening mechanisms—and consequently the propagation of microcracks through the soft phase with many path diversions—many deflections in the crack propagation path are observed in the micro- and macroscale (Fig. 4, E and F). Figure 5 shows that our composite possesses a strength similar to that of thermally tempered glass (3) but has a higher fracture toughness. Although our composite has a strength similar to the lower-range values of chemically strengthened glasses, it outperforms chemically tempered
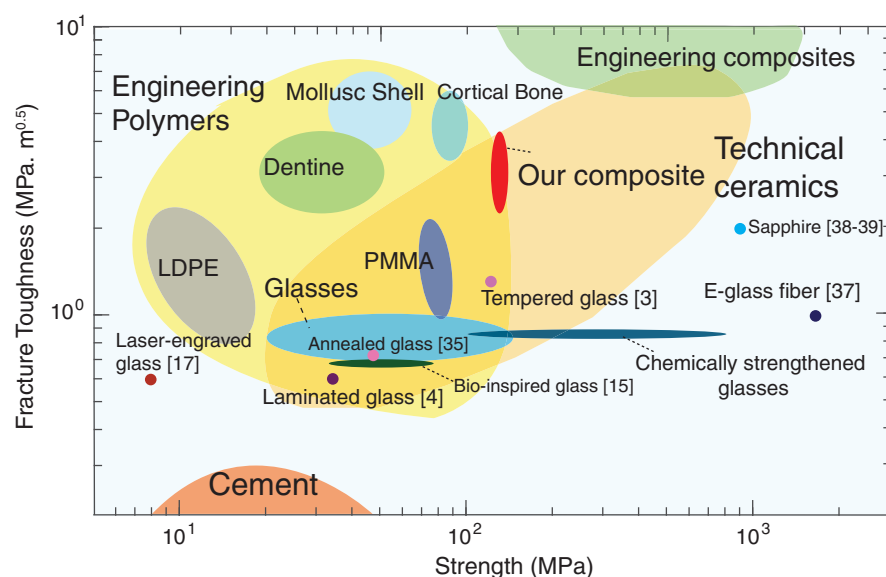

Fig. 5. Ashby plot of fracture toughness versus strength for numerous synthetic and natural materials. Our transparent nacreous composite (centrifuged at 2000g) outperforms annealed soda-lime (35), tempered (3), laminated (4), bioinspired transparent composite (15), and laser-engraved laminated (17) glasses in both strength and fracture toughness. E-glass fiber (37) and sapphire (38–39), as the best examples of glass and transparent ceramic materials respectively, outperform our composite in strength; however, unlike our material, they experience a brittle and catastrophic fracture. The data point representing our material's fracture toughness is made up of values starting from K_{IC} values and ending at the maximum K_{JC} values.

glasses in several key areas: (i) It possesses higher toughness values. (ii) Unlike chemically tempered glasses, it is possible to cut and machine our glass composite using conventional machining techniques and tools (fig. S10). (iii) Our material has a higher degree of damage tolerance, as the rising crack resistance curve (fig. S7C) demonstrates that any propagating crack will be met with increasingly strong resistance from the material, so these cracks will not compromise the overall strength of the system.

Our glass composite also outperforms previously reported bioinspired glass composites (15) in both strength and fracture toughness (fig. S7A). The reason for this difference is likely in the glass tablet aspect ratios. For a fixed matrix shear strength, there is a range of aspect ratios for tablets that causes the material to experience tablet pull-out (19). In this sense, too-short and too-long glass tablets cause vertical interface and tablet failure to be the prevailing modes of failure, respectively. In other words, keeping the interface shear strength constant while increasing the tablet aspect ratio would lead to a decrease in the WOF of the composite. The aspect ratio of the tablets in our material is about 25, or about one-tenth the size of the ones in (15), and closer to the ideal range for strength and toughness (eq. S14) (34), which explains the differences in strength and fracture toughness values of the two materials. Considering the WOF as a nonlinear measure of fracture

resistance, our composite outperforms annealed (35) and laminated glasses (4) as well as pure PMMA (fig. S8B). The laser-engraved laminated glass structure (17) possesses a very high WOF; however, this has only been achieved with a corresponding compromise in reduced material strength. Our material displays a brick-and-mortar microstructure (Fig. 2C and Fig. 4A) and produces high levels of fracture toughness because of its extrinsic toughening mechanisms, even though the volume fraction of the hard phase is lower than that observed in natural nacre (~95 vol % in natural nacre versus 46 vol % in our material). The lower content of the hard phase probably reduces tablet pull-out at large scales, resulting in our material being in the middle of the natural nacre's toughness range [J = 300 to 1700 J/m^2 for red abalone nacre (36)].

Hard-phase alignment has long been recognized as a key strategy, often pursued from a serialized bottom-up approach. Centrifugation is a rapid and scalable approach useful for fabricating any composite geometry and dimensions and may be further enhanced by increasing the density differential between hard and soft phases. This is a fundamental advantage over the serialized layer-by-layer approaches, which sacrifice production for precision. Additionally, this moves composite fabrication out of specialized nanofabrication facilities and into the realm of industrially approachable processes. The dependency of mechanical properties on centrifugation force

illustrates the importance of both aligning the hard phase tablets and minimizing the compliant PMMA phase in the overall composite structure, similar to the minimization of protein (~<5%) found in natural nacreous composites. This centrifugation-imposed order on the structure also effectively enables the activation of toughening mechanisms, such as crack deflection, tablet delamination, and tablet pull-out, which together contribute to high levels of fracture toughness in our material. These strategies enable our glass composite to mechanically outperform annealed, thermally tempered, and laminated glasses in fracture toughness and flexural strength. By making the soft and hard phases have the same refractive indices, one can create any number of varied materials in structured composites that have few to no optical defects.

REFERENCES AND NOTES

1. L. Wondraczek et al., Adv. Mater. 23, 4578–4586 (2011).
2. F. M. Ernsberger, Techniques of Strengthening Glasses, vol. 5 (Academic Press, Inc., 1980).
3. F. Petit, A. C. Sartieaux, M. Gonon, F. Cambier, Acta Mater. 55, 2765–2774 (2007).
4. X. Huang, G. Liu, Q. Liu, S. J. Bennison, Struct. Eng. Mech. 52, 603–612 (2014).
5. J. E. Minor, P. L. Reznik, J. Struct. Eng. 116, 1030–1039 (1990).
6. M. M. El-Shami, S. Norville, Y. E. Ibrahim, Alex. Eng. J. 51, 61–67 (2012).
7. H. S. Norville, K. W. King, J. L. Swofford, J. Eng. Mech. 124, 46–53 (1998).
8. H. D. Espinosa, J. E. Rim, F. Barthelat, M. J. Buehler, Prog. Mater. Sci. 54, 1059–1100 (2009).
9. F. Barthelat, H. Tang, P. D. Zavattieri, C. M. Li, H. D. Espinosa, J. Mech. Phys. Solids 55, 306–337 (2007).
10. N. Almqvist et al., Mater. Sci. Eng. C 7, 37–43 (1999).
11. H. Le Ferrand, F. Bouville, T. P. Niebel, A. R. Studart, Nat. Mater. 14, 1172–1179 (2015).
12. P. Podsiadlo et al., J. Phys. Chem. B 112, 14359–14363 (2008).
13. T. Ebina, F. Mizukami, Adv. Mater. 19, 2450–2453 (2007).
14. Y. Liu, S.-H. Yu, L. Bergström, Adv. Funct. Mater. 28, 1703277 (2018).
15. T. Magrini et al., Nat. Commun. 10, 2794 (2019).
16. M. Mirkhalaf, A. K. Dastjerdi, F. Barthelat, Nat. Commun. 5, 3166 (2014).
17. Z. Yin, A. Dastjerdi, F. Barthelat, Acta Biomater. 75, 439–450 (2018).
18. Z. Yin, F. Hannard, F. Barthelat, Science 364, 1260–1263 (2019).
19. M. R. Begley et al., J. Mech. Phys. Solids 60, 1545–1560 (2012).
20. P. Fratzl, O. Kolednik, F. D. Fischer, M. N. Dean, Chem. Soc. Rev. 45, 252–267 (2016).
21. F. Barthelat, R. Rabiei, J. Mech. Phys. Solids 59, 829–840 (2011).
22. F. Barthelat, J. Mech. Phys. Solids 73, 22–37 (2014).
23. T. S. Balke, thesis, McMaster University (1972).
24. T. P. Niebel, F. Bouville, D. Kokkinis, A. R. Studart, J. Mech. Phys. Solids 96, 133–146 (2016).
25. T. Hanemann, J. Boehm, C. Müller, E. Ritzhaupt-Kleissl, Proc. SPIE 6992, 69920D (2008).
26. J. Böhm, J. Hausselt, P. Henzi, K. Litfin, T. Hanemann, Adv. Eng. Mater. 6, 52–57 (2004).
27. L. M. Harwood, T. D. W. Claridge, Introduction to Organic Spectroscopy (Oxford Univ. Press, 1997).
28. X.-L. Gao, K. Li, Int. J. Solids Struct. 42, 1649–1667 (2005).
29. J. Zhang, T. Jin, Z. Wang, L. Zhao, Results Phys. 6, 265–269 (2016).
30. B. Lawn, Fracture of Brittle Solids (Cambridge Univ. Press, 1993).
31. ASTM Standard E1820-13, Standard Test Method for Measurement of Fracture Toughness (ASTM International, 2013); https://doi.org/10.1520/E1820-13.
32. A. P. Jackson, J. F. V. Vincent, R. M. Turner, Proc. R. Soc. Lond. B. 234, 415–440 (1988).
33. F. Barthelat, Z. Yin, M. J. Buehler, Nat. Rev. Mater. 1, 16007 (2016).
34. H. Gao, B. Ji, I. L. Jäger, E. Arzt, P. Fratzl, Proc. Natl. Acad. Sci. U.S.A. 100, 5597–5600 (2003).
35. S. M. Wiederhorn, J. Am. Ceram. Soc. 52, 99–105 (1969).
36. F. Barthelat, H. D. Espinosa, Exp. Mech. 47, 311–324 (2007).
37. M. Herráez, A. Fernández, C. S. Lopes, C. González, Phil. Trans. R. Soc. A. 374, 20150274 (2016).
38. G. E. Scott Jr., Angle Orthod. 58, 5–8 (1988).
39. Y. Mitamura, Y. Wang, J. Biomed. Mater. Res. 28, 813–817 (1994).

Science

Centrifugation and index matching yield a strong and transparent bioinspired nacreous composite

Ali AminiAdele KhavariFrancois BarthelatAllen J. Ehrlicher

A match made clear

The fabrication of strong and tough composites is of interest in many technologies, such as the combination of mechanical performance with transparency for robust display systems. Amini *et al.* combined and centrifuged glass flakes with poly(methyl methacrylate) (PMMA) to make a transparent composite. By doping the glass flakes, it was possible to alter the refractive index of PMMA to maximize optical clarity. Such composites show good strength and toughness and could have a wide range of potential applications as an alternative to current glass composites. —MSL

View the article online
https://www.science.org/doi/10.1126/science.abf0277
Permissions
https://www.science.org/help/reprints-and-permissions

Use of think article is subject to the Terms of service